

ok TC  
repete

## MEA - MODIFIED ENERGY AMPLIFIER PROPOSAL

S. A. Pereira and A. dos Santos

Instituto de Pesquisas Energeticas e Nucleares - IPEN/CNEN-SP  
Centro de Engenharia Nuclear - Div. de Física de Reatores  
P.O. Box 11049 (Pinheiros) - CEP: 05422-970  
Sao Paulo-SP-Brazil  
[sapercei@net.ipen.br](mailto:sapercei@net.ipen.br) ; [asantos@net.ipen.br](mailto:asantos@net.ipen.br)

### ABSTRACT

Recently Rubbia et al proposed a conceptual design of an Accelerator Driven System, known as Energy Amplifier (EA), as an advanced innovative reactor which utilizes a spallation neutron source induced by protons, from a Cyclotron or Linac, in a subcritical array imbedded in a liquid lead coolant. Besides of being converter and waste burner, the conceptual design generates energy and allows the use of Thorium as fuel. This paper introduces some qualitative and quantitative changes in the Rubbia's concept. The novel element of the proposal is the introduction of more than one spallation point in order to make the power density distribution more uniform and to reduce the requirements (current and energy) of the accelerator. Also, the subcritical core that in Rubbia's concept is hexagonal array of fuel pins imbedded in molten lead is replaced by a solid lead calandria cooled by Helium. The concept is referred to as MEA, Modified Energy Amplifier. The analyses reveal that the best option is to use three symmetric spallation sources. Moreover, the radial power peaking factor is less than 2.0 and the lead can be kept solid by an appropriate cooling design.

### 1. INTRODUCTION

To overcome the need of final storage, incineration of TRU is being considered by using fast neutrons from a spallation source [1], taking into account that the fission cross section is much higher than the capture cross section at this energies for most of TRU, and therefore transmuting long lived TRU in medium or short lived waste (FF). Besides the incineration of TRU's and FF, a coupled system consisting of spallation source and subcritical array of fuel, may have a positive gain of energy (net energy/energy to operate the accelerator). This fact has motivated innovative concepts of accelerator driven reactor in which thorium is being considered as fuel [2]. Rubbia et al [3] proposed a fast energy

amplifier (EA) using a three stage modular cyclotron of 1Gev, 12.5 mA to induce spallation with protons in liquid metal lead. The fuel in a hexagonal array of pin type forms the subcritical core surrounded the spallation source, and imbibed in liquid lead which circulates by natural convection. The conceptual design of Rubbia was proposed with a nominal power of 1500 MWth (670Mwe), a gain of 120, a high burnup (150GWD/t) and a reprocessing every 5 years. This paper introduces some qualitative changes in the Rubbia's concept such as more than one point of spallation, in order to reduce the requirement of proton energy and current of the accelerator, and mainly to make a flatter power density distribution. The subcritical core, which in the Rubbia's concept is an hexagonal array of pins immersed in a liquid lead coolant, is replaced by a concept of a solid lead calandria with the fuel elements in channels cooled by Helium. This concept allows the utilization of a direct thermodynamic cycle (Brayton), which is more efficient than a vapor cycle. These ideas do not violate the basic physics of the EA, but reduce the requirement in the accelerator complex, which is more realistic and economical in today accelerator technology. Finally, the utilization of *He* as coolant, compared to liquid *Pb*, is more realistic since the gas cooled reactor technology is well established and more efficient from the thermodynamic point of view, allowing simplification and the utilization in high temperature process like hydrogen generation.

## 2. THE MEA CONCEPT

The MEA fuel element design is shown in Fig. 1 while the conceptual design is shown in Fig. 2. The design constraints are a  $k_{eff}$  less than 0.97 in order to eliminate the need of safety rods [4], a radial peaking factor less than 2.0 and the maintenance of the lead between fuel elements solid. This lead will have a function to serve as a radiation shielding and a heat sink in case of accident. The spallation region will be made of liquid lead by an appropriate heating system. The fuel elements are cylindrical with a thermal barrier (or gap) to reduce the temperature in the fuel element border. There is also a second thermal barrier considering a He cooling pipe. This whole cooling design was able to keep the lead solid between fuel elements. One straightforward implication of the MEA conception is that the fuel elements are more separated than the usual design based on molten lead. This aspect will impose some extra requirements in the fuel load in order to keep  $k_{eff}$  around 0.97. The fuel rod characteristics and pitch (1.138cm) are the same of Rubbia's design. However, in order to keep a  $k_{eff}$  around 0.97 the number of fuel rods per element, and also its height, have to be increased. The final cylindrical fuel elements are filled with 433 fuel pins (0,1  $U^{233}$  +  $Th^{232}$ ) each one with  $88,3573\text{cm}^3$  and 200cm high.

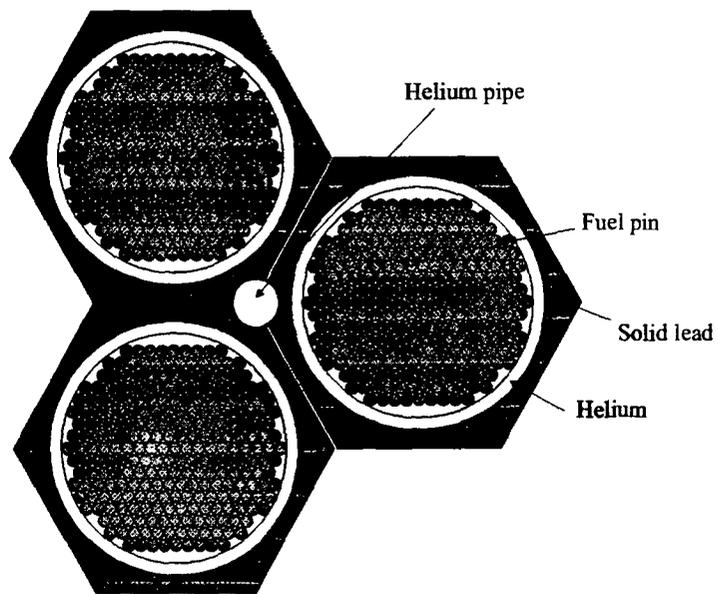


Figure 1. Cylindrical fuel element representation with a hexagonal fuel rod distribution

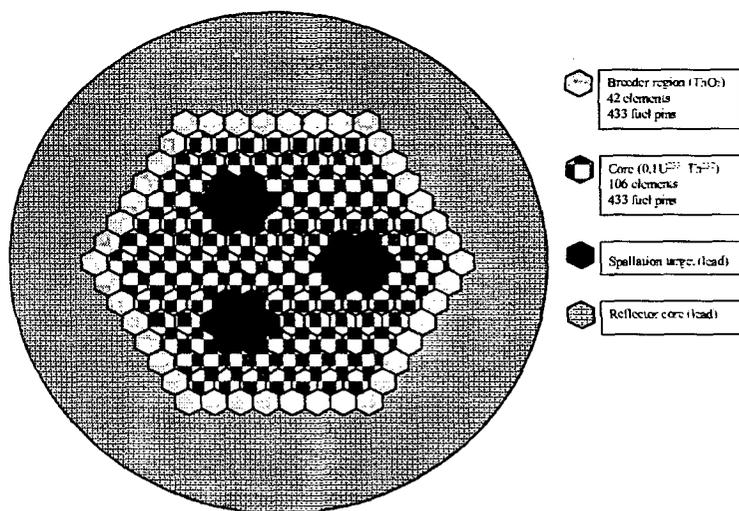


Figure 2. Alternative concept with 3 spallation regions.

### 3. METHODOLOGY AND CODE VALIDATION

The methodology employed in this work is shown in Fig. 3. It is based in a companion LAHET [5] and MCNP-4C [6] code systems. LAHET is the LANL version of the HETC Monte Carlo for the transport of protons. Its geometric transport capability is that of LANL's continuous energy neutron-photon Monte Carlo code MCNP-4C. The calculational methodology is made of two parts. In the first part LAHET performs the transport of protons and the subsequent characterization of the neutron and gamma sources arising from the spallation process in lead. For this purpose LAHET employs a Monte Carlo approach for the transport of protons through the lead target. The sources are written in special files denominated as NEUTP for neutrons and GAMTP for gamma for subsequent MCNP-4C utilization. Beyond that, LAHET has also the capability to calculate the energy deposited in the spallation region as well as the spallation products. The second part of the calculational methodology concerns the  $k_{\text{eff}}$  determination and the transport of neutrons and gamma through the fuel core and its surroundings. This task is accomplished by the continuous energy neutron-photon Monte Carlo code MCNP-4C. Given the geometric description of the problem, the material composition for each zone, and a nuclear data library describing the neutron and/or gamma interaction with matter, MCNP-4C solves the coupled neutron-gamma transport equation and calculates several responses or tallies such as  $k_{\text{eff}}$ , total energy deposited by neutrons and gamma in lead as well as several other quantities of importance in reactor analyses. The nuclear data needed for MCNP-4C are generated by NJOY [7] accessing the ENDF/B-VI nuclear data file.

The validations of the calculational methodology was made in three parts. The first part considers the characterization of the spallation neutron source itself. The second part considers the transport of the neutrons in the core and the power generated by fissions induced by  $^{232}\text{Th}$  and  $^{233}\text{U}$ . Also in this second part the quantity  $\epsilon$ , the ratio of the total neutron absorption in  $^{233}\text{U}$  to the neutron capture in  $^{232}\text{Th}$ , is determined for further analyses. The quantity  $\epsilon$  gives an indication of the equilibrium  $^{233}\text{U}$  concentration. The last part considers the ability of the calculational methodology to predict  $k_{\text{eff}}$  in critical systems consisting of  $^{233}\text{U}$  and  $^{232}\text{Th}$  and several related spectral ratios.

The first and second parts of the validation of the methodology were accomplished by comparing several calculated quantities with those published in Ref 3. Table 1 shows the neutron yield for the spallation process induced by high-energy protons calculated by LAHET code and also a comparison with those reported by Rubbia (FLUKA code [8]). Table 2 shows some results such as power, temperature etc., obtained by FLUKA and LAHET/MCNP-4C codes. The maximum cladding temperature is obtained from an unidimensional heat transfer model using the power density from either FLUKA or LAHET/MCNP-4C.

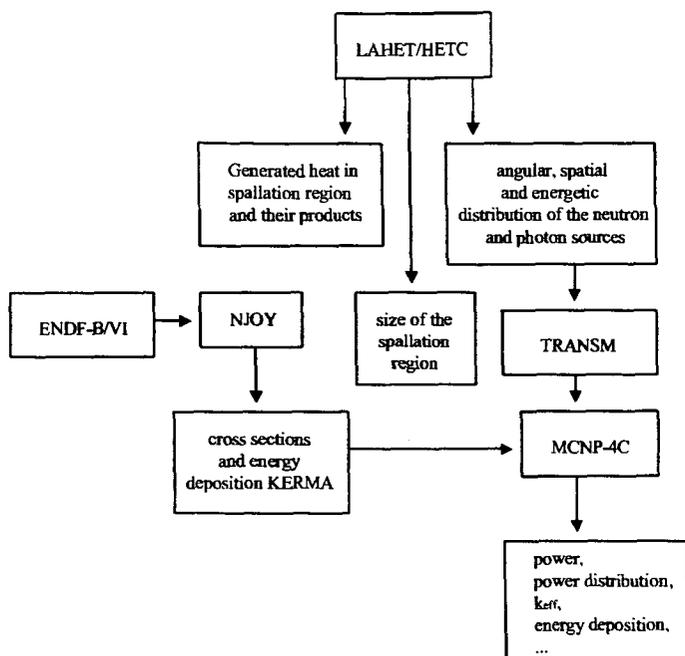


Figure 3. Methodology employed for MEA analyses.

Table I. Neutron yield for spallation process induced by high-energy protons calculated by LAHET and FLUKA.

Proton Energy (MeV)	Multiplicity $n_0$ , (n/p)		Integrated Yield $S_0$ , (n/seg.mA)	
	FLUKA	LCS	FLUKA	LCS
100	0.399	0.321	2.49E+15	2.00E+15
150	0.898	0.835	5.61E+15	5.21E+15
200	1.788	1.627	1.12E+16	1.02E+16
250	2.763	2.664	1.73E+16	1.66E+16
300	4.156	3.883	2.60E+16	2.42E+16
350	5.291	5.272	3.31E+16	3.29E+16
400	6.939	6.784	4.34E+16	4.23E+16
1000	----	28.76	----	1.79E+17

Table II. Comparison between EA results using FLUKA e LCS codes.

	FLUKA	LCS
Thermal power	1500 MW	1576 MW
$k_{eff}$	0.98	0.967
Specific power	52.8 W/g	53 W/g
Power density	523 W/cm <sup>3</sup>	527 W/cm <sup>3</sup>
$\epsilon$	0.11	0.107
Maximum cladding temperature	707 °C (Pb)	706 °C (Pb)

Tables I and II show very good agreement between LAHET/MCNP-4C predictions against those of FLUKA, thus enabling the calculational methodology of this work for the analyses of MEA.

In order to test and verify the reliability of <sup>233</sup>U and <sup>232</sup>Th isotopes nuclear data (part III), some benchmarks calculations were performed using the MCNP-4C code and ENDF/B-VI.5 library. The results of the simulated experiments THOR [9] and JEZEBEL [9] are summarized in Tables III and IV.

Table III. Results for the THOR experiment.

<i>Quantity</i>	<i>Experimental results</i>	<i>Calculated results</i>
Multiplication factor – $k_{eff}$	1,000 ± 0,001	0.9960 +/- 0.0030
$\sigma_f(\text{Th232})/\sigma_f(\text{U238})$	0,26 ± 0,01	0.2500 +/- 0.0040
$\sigma_{n,\gamma}(\text{Th232})/\sigma_{n,\gamma}(\text{U238})$	1,20 ± 0,06	1.2900 +/- 0.0004
$\sigma_{n,2n}(\text{Th232})/\sigma_{n,2n}(\text{U238})$	1,04 ± 0,03	1.0900 +/- 0.0040

Table IV. Results for the JEZEBEL experiment.

Experiment	Quantity	Experimental Result	Calculated Results
JEZEBEL23	$k_{eff}$	1.000 +/- 0.001	0.9945 +/- 0.00006
Case 11	$k_{eff}$	1,000 +/- 0,001	0.99326 +/- 0.0004
Case 21	$k_{eff}$	1,000 +/- 0,001	0.99536 +/- 0.0004
Case 22	$k_{eff}$	1,000 +/- 0,0011	0.99757 +/- 0.0004
Case 31	$k_{eff}$	1,000 +/- 0,001	0.99654 +/- 0.0004
Case 32	$k_{eff}$	1,000 +/- 0,001	0.99771 +/- 0.0004
Case 61	$k_{eff}$	1,000 +/- 0,0014	1.00134 +/- 0.0004

Again here, the calculational methodology was able to predict  $k_{eff}$  and several related spectral indices with a good accuracy, thus making it reliable for the MEA analyses.

### 3.1. LEAD TEMPERATURE

Another important quantity is the  $Pb$  temperature between fuel elements. Since the proposal here is to keep  $Pb$  solid, it must be guaranteed that the temperature next to fuel element is under the lead melting temperature ( $T_{fpb} = 328^\circ\text{C}$ ). For this purpose, an unidimensional model is employed to analyze the heat transfer phenomenon. The physical model concerns a medium (fuel elements) in a very high temperature where the heat is emitted by radiation. The fuel element gap is designed so that it can prevent practically the heat conduction to the surrounding lead. The heat that comes out of the fuel elements is conducted through the lead and reaches the second barrier where it is removed by a forced convection. The helium coolant has an average temperature of  $450^\circ\text{C}$ , an average pressure of 85 atm and a flow velocity of 8000 cm/sec. Fig. 4 shows schematically the physics involved for the determination of the lead temperature.

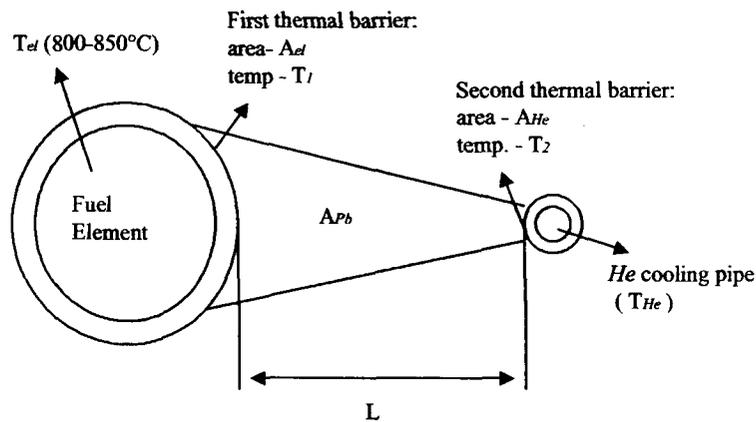


Figure 4. Schematic Lay Out for the Lead Temperature Determination.

Employing an unidimensional approach for the heat transfer phenomena, the equations are:

$$q = \sigma (T_{el}^4 - T_1^4) A_{el} \quad (\text{radiation})$$

$$q = k_{Pb} \frac{T_1 - T_2}{L} A_{Pb} \quad (\text{conduction})$$

$$q = h (T_2 - T_{He}) A_{He} \quad (\text{convection})$$

where:

$q$ - is the heat flux coming out of the fuel element,  
 $\sigma$ - is the Stefan-Boltzman constant,  
 $T_{el}$ - is the fuel element temperature,  
 $A_{el}$  – is the fuel element surface area,  
 $T_1$ - is the lead temperature at the fuel element surface,  
 $A_{pb}$ - is the lead area,  
 $k_{pb}$  – is the lead thermal conductivity,  
 $T_2$ - is the lead temperature at the He cooling pipe surface, and  
 $h$ - is the heat transfer coefficient.

Solving these equations  $T_1$  can be obtained in a straightforward fashion. From the Helium thermohydraulic conditions  $T_1$  was found to be 260°C which is lower than the lead melting point even considering a 20% uncertainty in the whole calculations.

#### 4. NEW CONCEPT RESULTS

##### 4.1 SPALLATION SOURCE CHARACTERIZATION AND THE ACCELERATOR WINDOW POSITIONING

The neutrons arising from the spallation process are produced in an extensive region and in an asymmetric way. Consequently, the characterization of the spallation source is of extreme importance for the MEA analysis. The first part of the MEA analysis was the determination of the size of the spallation region. Similarly to other similar systems [10,11], this study considers a cylindrical region for the spallation source. Following an extensive study changing the radius and the height of the cylinder, the conclusion reached is that the number of neutrons coming out of the source saturates after a specific radius and height. This work considers this source as a cylinder of radius equal to 62 cm and height equal to 150 cm. This spallation source occupies a volume of seven fuel elements.

The next part of the analysis is the positioning of the accelerator window as shown schematically in Fig. 5. The positioning of the accelerator windows is of the extreme importance to obtain an optimized power generation. In order to perform this task, several companion runs of the LAHET/MCNP-4C, as shown in Fig. 6, were performed. For each simulation the quantity calculated was the average number of the fissions per fuel rod and per incident proton. This quantity is proportional to the total power generated.

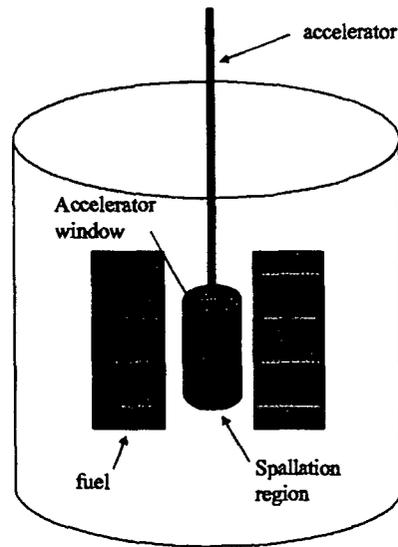


Figure 5. Artistic representation of the accelerator and the spallation target region (liquid lead).

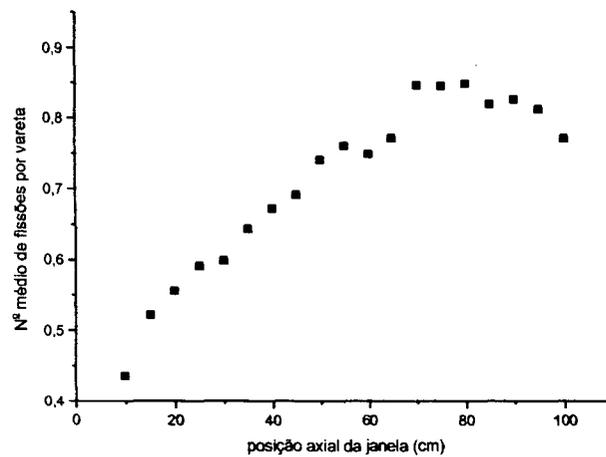


Figure 6. Average number of fissions per fuel rod versus the axial positioning of the accelerator window ( $E_p=500$  MeV).

Fig. 6 shows a maximum for the number of fissions per fuel at  $Z=80$  cm and the axial position referent to this maximum was chosen as the positioning of the accelerator windows for all calculations performed in this work.

Defined the size of the spallation source and the axial positioning of the accelerator window, the next step was to choose the number of the spallation sources for the MEA analysis. For this purpose, several analyses have been made with 1, 2, 3, 4 and 5 spallation sources. The configurations of these situations are shown in Fig. 7. The final results for these configurations are shown in Table V. One difficult present in all comparisons is the fact that  $k_{eff}$  is not constant. However, it can be partially corrected defining  $\Delta I$ , the source amplification variation, as:

$$\Delta I = \frac{1 - k_{eff}}{1 - k_{effr}} \quad (1)$$

were  $I$  is the source amplification,  $k_{eff}$  is the multiplication factor for the case under consideration and  $k_{effr}$  is the value for the reference  $k_{eff}$  which is calculated with a source in the central region. Multiplying the power by  $\Delta I$ , one can eliminate partially the  $k_{eff}$  dependence. Table V shows these aspects. There is little variation of the power for the cases of 2, 3, 4 and 5 spallation sources.

Table V.  $k_{eff}$  and Power Considering 1, 2, 3, 4 and 5-spallation sources.

<i>Number of spallation sources</i>	<i><math>k_{eff}</math></i>	<i>Power (MWth/mA)</i>	<i>Power corrected by <math>\Delta I</math></i>
1	0,96410	44,08	44,08
2	0,96242	31,14	32,59
3	0,94632	21,61	32,32
4	0,93598	17,44	31,09
5	0,90197	10,82	29,55

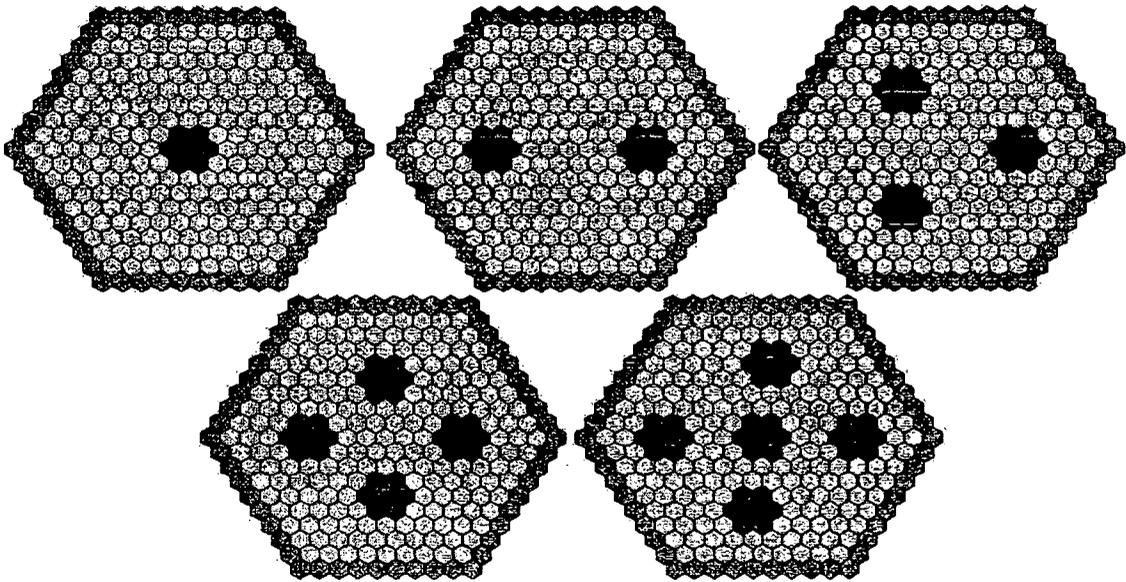


Figure 7. Representative Lay-Out for the Configurations of 1,2,3,4,5 Spallation Sources.

The choice of the 3 sources configuration was made due to the fact that, when compared to the 4 and 5 source configurations, it presents higher power, a symmetric distribution of the sources over the core, and less accelerators, resulting in lower costs with maintenance, investment and electric consume. When compared with the 2 source configuration, the main advantage is the symmetric distribution over the core.

### 4.3 RADIAL POWER DISTRIBUTION

For the final configuration for the MEA proposal, 3 regions of spallation, several analysis have been performed considering the radial position of the sources, number of the fuel rings (core size), and consequently, the quantity of the fuel elements and also the utilization of the fuel elements with different fissile masses. The results were compared to those of the configuration of one central spallation source, which is the reference for all the analyses. The characteristics for each configuration and the calculated quantities are given in Table VI.

Considering first the radial power peaking factor for each element, one must realize that due to the symmetry of the problem it is not necessary to calculate this quantity for all fuel elements. Furthermore, for the radial power peaking factor it is necessary to calculate the radial power distribution only along the black line as shown in Fig. 8 which is the most critical one; i.e. with the highest radial power. This aspect simplifies considerably the analyses, because decreases significantly the MCNP-4C CPU time of each configuration. All the analyses considered the proton energy equal to 500MeV. Fig. 9 shows the radial power distribution along the “black line” of Fig. 8 for each configuration considered in this work.

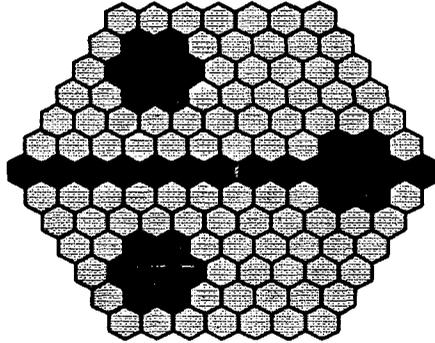


Figure 8. Schematic representation for the radial power determination.

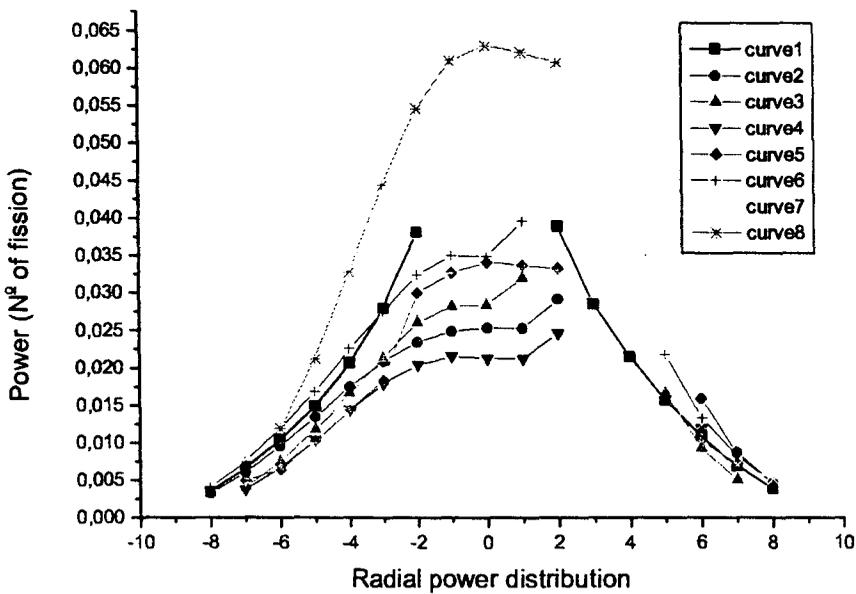


Figure 9. Radial power distribution for different configurations (total processing time: 20395min (14,16days)).

In order to explain each configuration, Fig. 10 shows the descriptive legend used in Fig. 11. For each configuration, the quantities calculated are: the average number of fissions per fuel rod per incident proton, the average numbers of fissions per fuel element, the radial power peaking factor and  $k_{eff}$ .

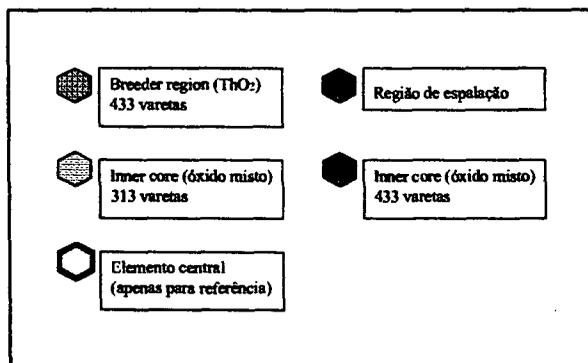


Figure 10. Descriptive legend for Figure 11.

Before the discussions of the configurations properly consider some details related to positioning of the sources in the core. Fig. 12 shows  $k_{eff}$  and the total power for a three-source configuration as these sources starting from the central region move toward the board. Considering  $k_{eff}$  first, this quantity decreases up to position 2 as the sources moves away from the center and decreases afterwards. In this case, for positions 1 and 2, the fact of substituting 21 elements for lead ( the first three regions of spallation) influences more than the the addition of a few fuel elements at the center. From position 3 on, the fuel mass in the central region begins to be predominant for the multiplication. Considering the power, this quantity decreases up to position 2 due to the  $k_{eff}$  decreases , increases up to position 4 due to the  $k_{eff}$  increase and decreases after that because the sources are too close to the border and the neutron leakage gets high. This exercise shows the complexity of the positioning of the sources for maximizing the power. The next topics will add some insight of the problem when the radial peaking factor has to be minimized.

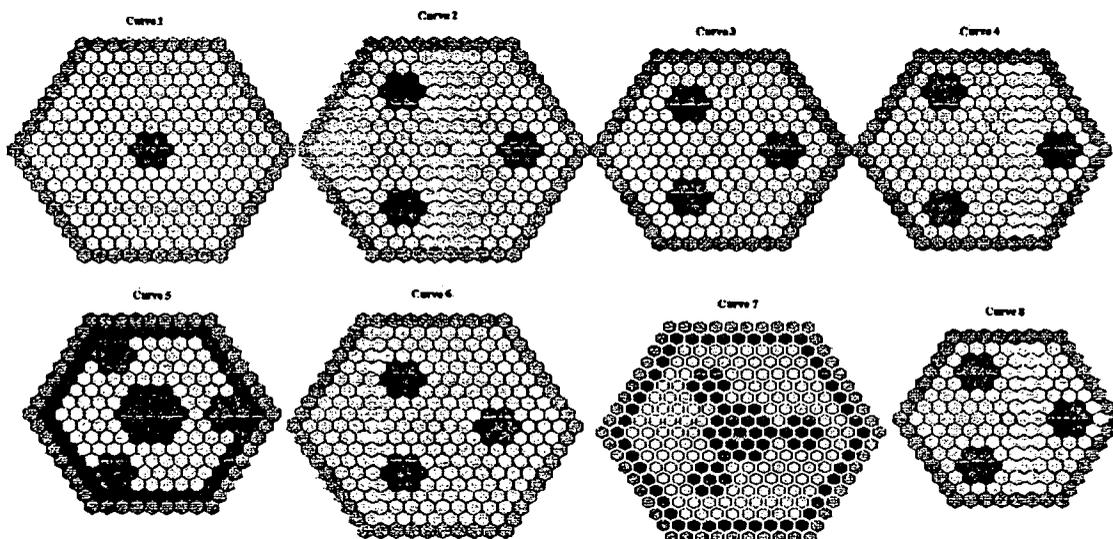


Figure 11. Schematic Representation of the Configuration Considered for MEA Analyses

Table VI. Calculated Characteristics for Each Configuration.

	CURVE1	CURVE2	CURVE3	CURVE4	CURVE5	CURVE6	CURVE7	CURVE8
Average N <sup>2</sup> of fissions per fuel pin over the core	3.18	2.78	2.19	1.99	2.20	3.24	3.82	3.63
Average N <sup>2</sup> of fissions per fuel pin over the core per fuel element	0.0054	0.0142	0.0148	0.0134	0.0149	0.0165	0.0195	0.0340
Peaking Factor	7.19	2.06	2.16	1.83	2.29	2.39	2.98	1.85
k <sub>eff</sub>	0.947	0.955	0.937	0.942	0.952	0.947	0.961	0.965
Config.	1 source pos. 0 7 rings 196 elem. (313 pins)	3 sources pos. 4 7 rings 196 elem. (313 pins)	3 sources pos. 3 6 rings 148 elem. (313 pins)	3 sources pos. 4 6 rings 148 elem. (313 pins)	3 sources pos. 4 6 rings 148 elem. 2 distinct fuel regions	3 sources pos. 3 7 rings 196 elem. (313 pins)	3 sources pos. 3 7 rings 196 elem. 2 distinct fuel regions	3 sources pos. 3 5 rings 106 elem. of bigger diameter (433 pins)

The configuration for curve 1 is the reference for all configurations. The spallation source is placed in the central position and the configuration has 7 rings of the fuel elements. The radial power peaking factor is the worst of all. In fact the main concern of this work is to propose a solution to minimize this peaking factor. The configuration referent to curve 2 shows the three-spallation sources placed in position 4 considering the same amount of fuel elements. The only difference between configuration 2 and 6 is the position of the spallation sources. Comparing these two configurations, it can be noted that there is a decrease of the power due to the fact that the sources are close to the border, but an improvement in the power peaking factor. The  $k_{eff}$  is slightly higher for configuration 2 because there is more fuel at the central region. The immediate conclusion that can be drawn from configurations 2 and 6 is that as the sources moves toward the power and the radial peaking factor decrease. The configuration of curve 3 considers again the sources placed in position 3, but in this case there are only 6 rings of fuel elements for a total of 148. The decrease of the power compared to configuration 1 and 2 is due mainly to the decrease of  $k_{eff}$ . This core has less fuel mass. Comparing configuration 1 and 3 it can be noted that the radial power peaking factor improves. Consequently, a smaller core implies in a smaller radial peaking factor. The configuration for curve 4 considers now the sources placed in position 4. There is a slight decrease of the power although  $k_{eff}$  is higher. Again here, the neutron leakage overwhelms the increase on  $k_{eff}$  and the net effect is a decrease on the power. As in the case of configuration 2 and 6 the radial peaking factor improves as the sources move away from the center. In curve 5, the sources are still placed in position 4

and the core has also 148 fuel elements. In this case the purpose is to improve performance of the core relatively to configuration 4. For this goal, the fuel mass has been increased in the central region to achieve a better  $k_{eff}$  and consequently the power. The power improves but the peaking factor worsens. The configuration of curve 6 has the three spallation sources placed in position 3 and seven rings of fuel elements for a total of 196. In configuration 7 the spallation sources are placed in position 3. There are 7 rings of fuel elements, and like configuration 5, the central region has a bigger quantity of fuel mass in order to improve the  $k_{eff}$  and consequently the power. Again here the power improves but the peaking factor worsens. Finally, the configuration for curve 8 considers again the sources placed in position 3 but the core has 5 rings of fuel elements for a total of 106. In this case the fuel mass was increased equally in the all core by means the increase of the fuel element diameter.

In this phase, one choice must be made. Either the total power or a flatter radial power distribution is privileged. The best configurations were 7 and 8. In both configurations the spallation sources were placed in position 3 and have a  $k_{eff}$  around 0.96. The configuration 8 was chosen because it is more compact, it has less fuel mass, which results in a better power distribution factor.. The configuration 7 has a peaking factor of 2.98, while the configuration 8 has a peaking factor of 1.85, which is much less than the requested value of 2.0. The radial power density distribution for the final proposal is shown in Fig. 13.

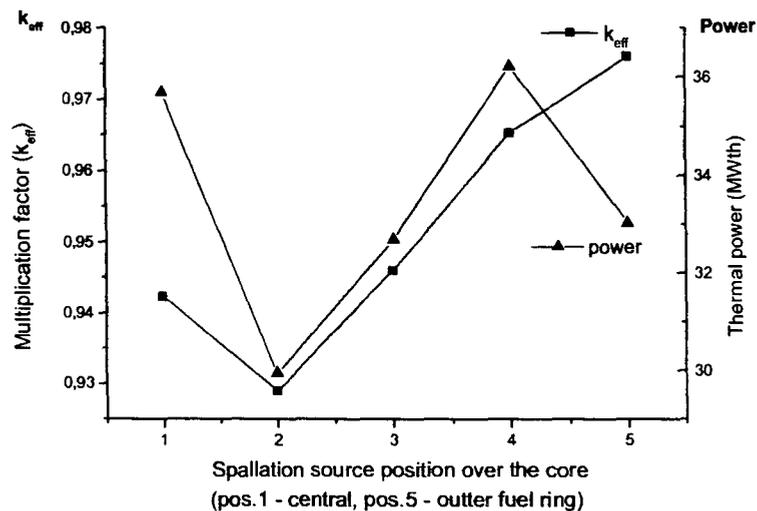


Figure 12.  $K_{eff}$  and Power as a function of the radial source positions.

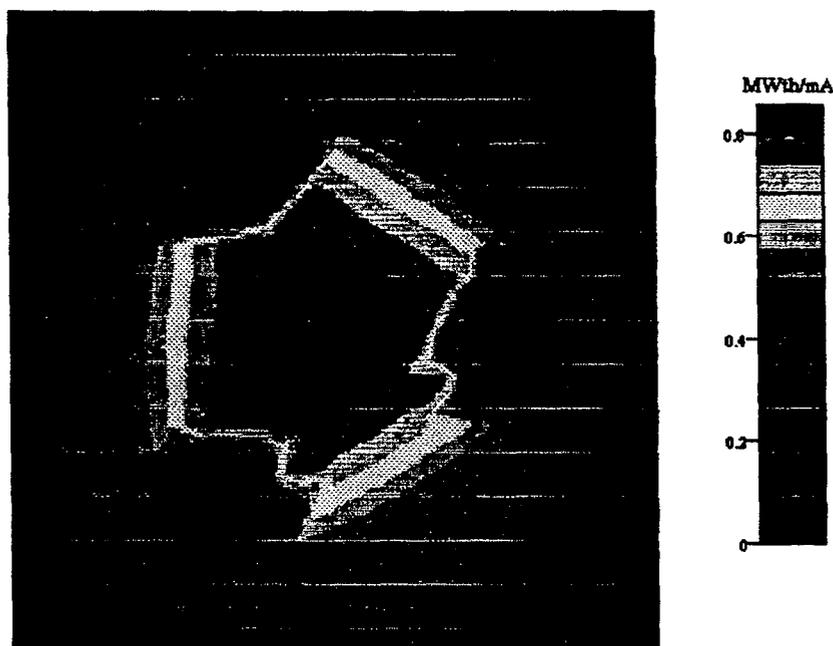


Figure 13. The radial power density distribution for the final MEA proposal with 3 spallation sources. All the quantities are per fuel element (total processing time: 49005min (34,03days)).

To obtain these results, the calculations took several days of processing time. Since the core is a hexagonal array, and the spallation source distribution is symmetric, the calculations simulated only one third of the core and the values were reflected for the other symmetric regions, resulting then a processing time of around 34 days.

One can note the three blue islands representing the three-spallation regions, and the central red region indicating the higher heat generation (energy). It also can be noted that the radial power distribution is symmetric due to the fact that was 3 spallation sources have been used.

## CONCLUSIONS

The analyses of MEA has been successfully accomplished. The calculational methodology utilized in this work reproduces with good accuracy the benchmark results. Even for the  $^{232}\text{Th}$  and  $^{233}\text{U}$  systems which are considered systems that did not receive too much attention from the nuclear data community, their nuclear data are of reasonably good quality as evidenced in the benchmark analyses. In order to keep the lead between fuel elements solid, the cooling design system using pipes with helium between the fuel elements was able to guarantee that the temperature stays below the limit. The proposed conception considering protons of 500MeV possesses a gain of 70 and the total thermal power per 3 mA is 105 MWth. For protons of 1 GeV the total power per 3 mA is 303

MWth and the gain is 120. Finally, using a three spallation source configuration a radial power peaking factor achieved is less than 2 which is great improvement compared to 7, in the case of a central spallation source configuration.

## ACKNOWLEDGEMENTS

The authors are grateful to LCCA (Laboratório de Computação Científica Avançada – USP) for providing the computational resource for this work.

## REFERENCES

1. C. Rubbia et alii, "A Realistic Plutonium elimination scheme with fast energy amplifiers and Thorium-Plutonium fuel". CERN/AT/95-53 (ET), 1995.
2. C. Rubbia et alii, "Fast neutron incineration in the energy amplifier as alternative to geologic storage: The case of Spain". CERN/LCH/97-01 (EET), 1997.
3. C. Rubbia, et al: *Conceptual design of a fast neutron operated high power energy amplifier*. CERN/AT/95-44 (ET). 1995.
4. Gudowsky, W. et al., "Accelerator-driven Transmutation Projects in Sweden in a European Perspective", proceedings of Technical Working Group on Fast Reactors (TWG-FR), Almaty/Kurchatov, Kazakhstan, 14-18 May 2001.
5. R. E. Prael and H. Linchtenstein, "User Guide to LCS: The Lahet Code System". LA-UR-89-3014, Los Alamos National Laboratory, 1989.
6. Briesmeister, Judith F., editor, "MCNP – A General Monte Carlo Code for Neutron and Photon Transport", LA-7396-M Revision 2, Los Alamos National Laboratory (September 1986).
7. MacFarlane R. E., Muir D. W. and Boicourt R. M.: "The NJOY Data Processing System, Volume II: The NJOY, RECONR, BROADR, HEATR, and THERMR Modules. Report LA-9303-M, Vol. II (ENDF-324), 1982.
8. FLUKA: Status and Prospective for Hadronic Applications, A. Fasso, A. Ferrari, J. Ranft, P.R. Sala, proceedings of the MonteCarlo 2000 Conference, Lisbon, October 23-26 2000, A. Kling, F. Barao, M. Nakagawa, L. Tavora, P. Vaz eds., Springer-Verlag Berlin, p. 955-960 (2001).
9. "Cross Section Evaluation Working Group Benchmark Specification", ENDF-202 (BNL-19302), Brookhaven National Laboratory.
10. Letourneau, A. et al., "Neutron production in bombardments of thin and thick W, Hg, Pb targets by 0.4, 0.8, 1.2, 1.8 and 2.5 GeV protons", Nucl. Instr. and Meth. B, 170 (2000) 299-322.
11. Rubbia, C.; Rubio, J. A.; Buorno, S.; Carminati, F.; Fiétier, N.; Galvez, J.; Gelès, C.; Kadi, Y.; Klapisch, R.; Mandrillon, P.; Revol, J. P. and Ch. Roche. "Conceptual Design of a Fast Neutron Operated High Power Energy Amplifier". European Organization for Nuclear Research CERN/AT/95-44(ET), 1995.



# CENTRO DE ENGENHARIA NUCLEAR

## CENF

### MEA – Modifeid Energy Amplifier Proposal

PHYSOR-2002, Int. Conf. on the new Frontiers of Nuclear Technology: Reactor Physics, Safety and High Performance Computing, Seoul, Korea, 7-10 October 2002.

Artigo Científico

ENS.CENF.CPG.031

ARTC.002.00

AUTOR	Rubrica	Data	VERIFICADOR	Rubrica	Data
Sergio Anéfalos Pereira	<i>P/A.J.</i>	04/11/02	<i>Adimir</i>	<i>A.J.</i>	<i>04/11/02</i>
Adimir dos Santos	<i>A.J.</i>	04/11/02			

APROVAÇÕES			Rubrica	Data
Chefe de Área	Adimir dos Santos		<i>A.J.</i>	<i>04/11/02</i>
Lider	Adimir dos Santos		<i>P.J.</i>	<i>04/11/02</i>
Gerente do Centro	Antonio Teixeira e Silva		<i>ATS</i>	<i>11/11/02</i>

ARQUIVO			

TC  
marta

IPEN/CNEN-SP  
BIBLIOTECA  
"TEREZINE ARANTES FERRAZ"

Formulário de envio de trabalhos produzidos pelos pesquisadores do IPEN para inclusão na  
Produção Técnico Científica

AUTOR(ES) DO TRABALHO:

Sergio Alexandre Pereira, Adilson dos  
Santos

LOTAÇÃO: CENF

RAMAL: 3338

TIPO DE REGISTRO:

art. periód.:  
cap. de livro

Publ. IPEN  
Art. conf

resumo  
outros  
(folheto, relatório, etc...)

TITULO DO TRABALHO:

MEA - Modified Energy Amplifier  
Proposal.

APRESENTADO EM: (informar os dados completos - no caso de artigos de conf., informar o título  
da conferência, local, data, organizador, etc...)

PHYSOR-2002, Int. Conf. on the New Frontiers  
of Nuclear Technology: Reactor Physics, Safeguards,  
and High Performance Computing, Seoul, Korea, 7-10 October 2002

PALAVRAS CHAVES PARA IDENTIFICAR O TRABALHO:

Spallation, Energy Amplifier, Hybrid System,  
Plutonium

ASSINATURA: Adilson dos Santos

DATA: 04 / 11 / 2002

179 NOV 2002